Fusion of ^{6}Li with ^{159}Tb at near-barrier energies

M. K. Pradhan, A. Mukherjee,[*] P. Basu, A. Goswami, R. Kshetri, Subinit Roy, P. Roy Chowdhury, and M. Saha Sarkar
Nuclear Physics Division, Saha Institute of Nuclear Physics, 1/AF, Bidhan Nagar, Kolkata-700064, India

R. Palit
Department of Nuclear & Atomic Physics, Tata Institute of Fundamental Research, Mumbai-400005, India

V. V. Parkar and S. Santra
Nuclear Physics Division, Bhabha Atomic Research Centre, Mumbai-400085, India

M. Ray
Department of Physics, Behala College, Parnasree, Kolkata-700060, India
(Received 5 May 2011; published 13 June 2011)

Complete and incomplete fusion cross sections for ^{6}Li + ^{159}Tb have been measured at energies around the Coulomb barrier by the γ-ray method. The measurements show that the complete fusion cross sections at above-barrier energies are suppressed by ∼34% compared to coupled-channel calculations. A comparison of the complete fusion cross sections at above-barrier energies with the existing data for ^{11,10}B + ^{159}Tb and ^{7}Li + ^{159}Tb shows that the extent of suppression is correlated with the α separation energies of the projectiles. It has been argued that the Dy isotopes produced in the reaction ^{6}Li + ^{159}Tb at below-barrier energies are primarily due to the d transfer to unbound states of ^{159}Tb, while both transfer and incomplete fusion processes contribute at above-barrier energies.

DOI: 10.1103/PhysRevC.83.064606 PACS number(s): 24.10.Eq, 25.70.Jj, 25.60.Pj, 25.70.Mn

I. INTRODUCTION

Near-barrier fusion is governed by the structure of the interacting nuclei and the coupling to the direct nuclear processes, such as inelastic excitation and nucleon transfer [1,2]. For nuclear systems with tightly bound nuclei, the coupling of the relative motion to these internal degrees of freedom successfully explains the enhancement of fusion cross sections with respect to the one-dimensional (1D) barrier penetration model (BPM) calculations at sub-barrier energies [2]. However, the situation gets more complicated in reactions involving weakly bound nuclei, since they may break up prior to fusion. The interest in understanding the influence of breakup on fusion and other reaction processes has indeed received a fillip in recent years, especially because of the recent advent of radioactive ion beam facilities in different laboratories around the world.

Owing to the low intensities of the radioactive ion beams currently available, experimental investigation of reaction mechanisms with unstable beams is still difficult, though measurements are being increasingly reported [3–11]. In contrast, precise fusion cross-section measurements can be carried out with the readily available high-intensity beams of weakly bound stable nuclei, ^{6,7}Li and ^{9}Be, which have significant breakup probabilities. Such studies with weakly bound stable projectiles may serve as an important step toward the understanding of the influence of breakup on fusion processes.

During the past few years, the effect of the breakup of weakly bound nuclei on the fusion process has been extensively investigated. In fusion measurements of weakly bound stable projectiles with heavy targets [11–22], events corresponding to the complete fusion (CF) of the projectile with the target could be separated experimentally from those due to the incomplete fusion (ICF) process (where part of the projectile is captured by the target). The literature shows that the CF cross sections are substantially suppressed at above-barrier energies, compared to the predictions of the 1D BPM calculations. This has been attributed to the breakup of the weakly bound projectiles prior to reaching the fusion barrier.

In contrast, in fusion measurements for medium- and light-mass systems [23–31], where CF and ICF products could not be experimentally distinguished, only total fusion (CF + ICF) cross sections were measured. Such measurements show that the breakup has no significant effect on the total fusion at above-barrier energies.

Systematic fusion excitation function measurement carried out by the characteristic γ-ray method, for the systems ^{10,11}B + ^{159}Tb and ^{7}Li + ^{159}Tb [19], shows that the CF cross sections at above-barrier energies are suppressed for the systems ^{10}B + ^{159}Tb and ^{7}Li + ^{159}Tb by ∼14% and ∼26%, respectively, with respect to the coupled-channel (CC) calculations. Also, CF suppression was found to be correlated with the α breakup threshold of the projectiles. In the context of these results, it appears worthwhile to measure the CF cross sections for the system ^{6}Li + ^{159}Tb, in view of the fact that ^{6}Li has the lowest α breakup threshold (1.45 MeV) among the stable projectiles ^{6,7}Li, ^{9}Be, and ^{10,11}B. The present work

[*]anjali.mukherjee@saha.ac.in

deals with the measurement of CF and ICF cross sections for ^{6}Li + ^{159}Tb at energies around the Coulomb barrier, using the γ-ray method. To check the consistency of the present results with those of Ref. [19], the reaction ^{7}Li + ^{159}Tb was repeated at a few energies in the present work. Some preliminary results of the measurement have been reported in conference proceedings [32].

II. EXPERIMENTAL DETAILS

The experiment was performed using the 14UD BARC-TIFR Pelletron accelerator at Mumbai. Beams of ^{6}Li in the energy range 23–39 MeV and ^{7}Li at energies of 28, 34, and 37 MeV bombarded a self-supporting ^{159}Tb foil of thickness 1.59 ± 0.08 mg/cm^2. To monitor the beam and also for normalization purposes, two Si-surface barrier detectors were placed at $\pm 30^\circ$ about the beam axis inside a spherical reaction chamber of 22 cm diameter. The total charge of each exposure was measured in a 1-m-long Faraday cup placed after the target. The γ rays emitted by the reaction products were detected in an absolute efficiency calibrated Compton suppressed clover detector, placed at $+125^\circ$ with respect to the beam direction. A high-purity germanium (HPGe) detector having a Be window was placed at -125° with respect to the beam direction, mainly to detect low-energy γ rays. Both online and offline γ spectra were taken during the runs, using the Linux-based data acquisition software LAMPS [33]. The absolute efficiencies of the γ-ray detectors were determined using the standard calibrated radioactive sources (^{152}Eu, ^{133}Ba, ^{209}Bi, ^{60}Co, ^{137}Cs) placed at the same geometry as the target. The target thickness was determined using the 137.5 keV [$7/2^+ \rightarrow 3/2^+$ (g.s.)] Coulomb excitation line of ^{159}Tb. The same target was used for all beam exposures. In order to minimize the accumulation of radioactivity in the target, target irradiation was carried out from the lowest beam energy upward. A typical γ-ray addback spectrum from the clover detector, at the bombarding energy of 39 MeV, is shown in Figs. 1(a) and 1(b). The nuclei produced in the reaction were identified by their characteristic γ-ray energies and are labeled in the figure.

III. DETERMINATION OF COMPLETE FUSION YIELDS

The compound nuclei ^{165}Er and ^{166}Er formed following the CF of ^{159}Tb with ^{6}Li and ^{7}Li, respectively, decay predominantly by neutron evaporation. This is also predicted by statistical model calculations using the code PACE [34]. In the measured energy range the evaporation of two to five neutrons occurs, resulting in the formation of $^{163\text{-}160}$Er and $^{164\text{-}161}$Er evaporation residues (ERs) for the reactions ^{6}Li + ^{159}Tb and ^{7}Li + ^{159}Tb, respectively.

In determining the ER cross sections, the online spectra were mostly used. But as and when required, the offline spectra were also used. It needs to be mentioned here that in situations where the ERs are stable, only the in-beam γ-ray spectroscopy method can be used. However, in cases where unstable ERs undergo further radioactive decay to populate the excited states of their daughter nuclei, which in turn decay to their ground states by emitting γ rays, one can also use the off-beam γ-ray method, if the situation is favorable. In the present work, this could be done only for the $4n$ channel residual nucleus, ^{161}Er with a half-life ($T_{1/2}$) of 3.21 h, produced in the reaction ^{6}Li + ^{159}Tb. The off-beam γ-ray method could not be used for the ER ^{163}Er ($T_{1/2} = 75$ mins), as 99.9% of ^{163}Er undergoes electron-capture (EC) decay to a ground state of ^{163}Ho. Also, as the same target was used for all the irradiations, the off-beam method could not be used for the ER ^{160}Er, having $T_{1/2} =$ 28.58 h, which is substantially large compared to the data accumulation times (typically ∼1–2 h).

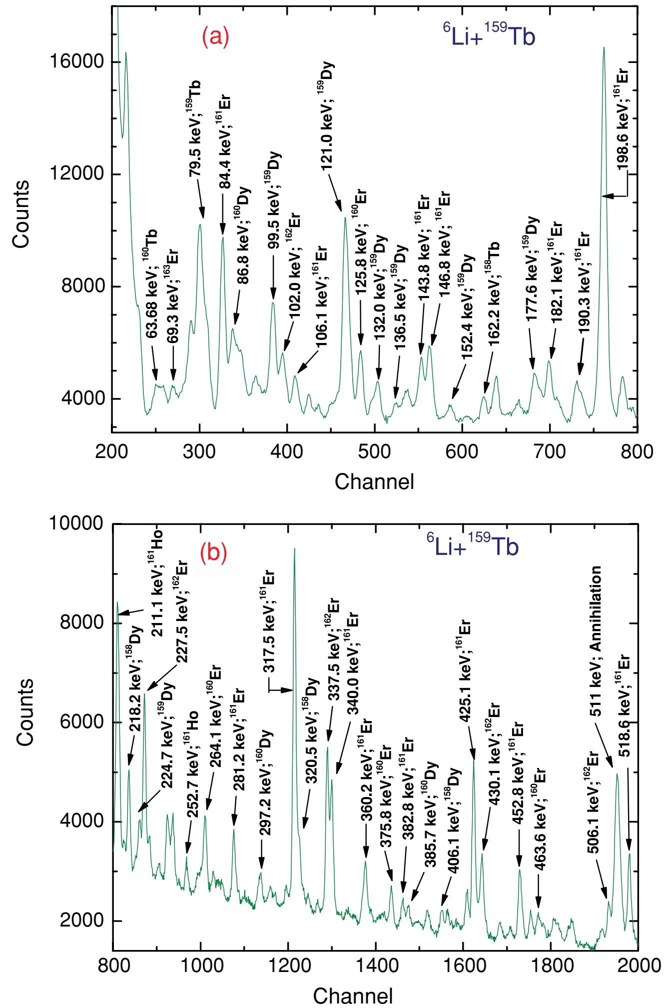

FIG. 1. (Color online) Typical γ-ray spectrum obtained with a clover detector placed at 125°, for the reaction ^{6}Li + ^{159}Tb, at a bombarding energy of 39 MeV.

While analyzing the data from the clover detector, the addback spectra were used. Wherever possible, the cross sections obtained from the clover-detector spectra were compared with those from the HPGe-detector spectra, and they were found to be in good agreement.

The γ-ray cross sections (σ_γ) were obtained from the relation

$$\sigma_\gamma = \frac{N_\gamma}{(\epsilon_\gamma N_B N_T)}, \quad (1)$$

where N_γ is the number of counts under the γ-ray peak, ϵ_γ is the absolute full energy peak detection efficiency of the detector for the specific γ ray, N_B is the total number of beam particles incident on the target, and N_T is the number of target nuclei per cm^2. The quantity N_B was determined by dividing the charge Q collected in the Faraday cup by the equilibrium charge value $\bar{Z}e$, obtained from Ref. [35]. The total systematic uncertainty in the γ-ray cross sections, arising because of the uncertainties in N_B, N_T, and ϵ_γ, is ~8%. This is added in quadrature to the statistical error in N_γ to get the total error in σ_γ.

For the even-even ERs (^{164,162,160}Er), the cross sections were extracted from the extrapolated value of the intensity at $J = 0$ obtained from the measured γ-ray intensities (after correcting for the internal conversion) for various transitions in the ground-state rotational band [19]. For the odd-mass ERs (^{163,161}Er) the cross sections were obtained by adding the cross sections of the γ rays corresponding to the transitions from the excited states to the ground states of the nuclei, as done by Broda *et al.* [36]. In such cases, however, direct population of the ground states of the nuclei could not be considered. Nevertheless, a direct feed to the ground states is expected to be substantially small in this mass and energy region, except at very low bombarding energies. In fact, in the present work this has been checked for the ER ^{161}Er, produced in the reaction ^{6}Li + ^{159}Tb, as both the in-beam and off-beam γ-ray methods could be applied to measure its production cross sections at low bombarding energies. It was observed that the cross sections, obtained from the in-beam γ rays of ^{161}Er (where direct population of the ground state is not included) and those from the off-beam γ rays of ^{161}Ho, following EC decay of ^{161}Er (which obviously includes the direct ground-state population of ^{161}Er), are practically the same. This shows the ground-state contribution to be rather small and it can safely be ignored in the evaluation of the CF cross sections. The CF cross sections for both reactions were obtained from the sum of the $2n$–$5n$ ER cross sections.

Figure 2 shows the individual xn channel cross sections normalized to the CF cross sections (fractional channel cross sections) for the reaction ^{6}Li + ^{159}Tb. The measured CF cross sections, along with the total errors, for the reaction ^{6}Li + ^{159}Tb are plotted in Fig. 3. The CF cross sections for ^{7}Li + ^{159}Tb, measured at a few bombarding energies in the same setup, are seen to agree well with the earlier measurements [19,36], thus enabling a reliable comparison of the present results with the earlier ones.

IV. COUPLED-CHANNEL CALCULATIONS

To interpret the measured fusion excitation function in a theoretical framework, the realistic coupled-channel (CC) code CCFULL [37] was used to calculate the fusion cross sections for ^{6}Li + ^{159}Tb. The initial input potential parameters (V_0, r_0, and a) were obtained from the Woods-Saxon parametrization of the Akyüz-Winther (AW) potential [38], and are shown in Table I. The table also shows the corresponding uncoupled fusion-barrier parameters (V_b, R_b, and $\hbar\omega$). As CCFULL cannot handle shallow potentials, a deeper potential was used.

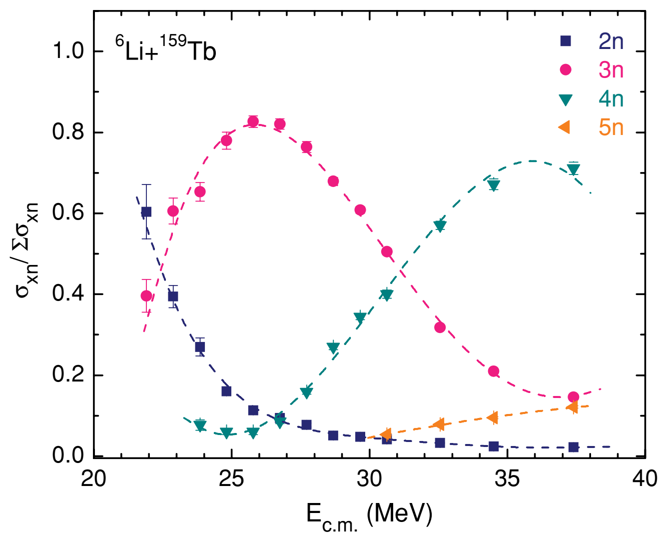

FIG. 2. (Color online) Ratio of individual channel cross sections to the total channel cross sections as a function of the center-of-mass energy for the reaction ^{6}Li + ^{159}Tb. The errors are statistical only. The dashed lines are drawn to guide the eye.

This modified potential was derived keeping the diffuseness parameter fixed at $a = 0.85$ fm, following the systematic trend of high diffuseness required to fit the high-energy part of the fusion excitation functions [39]. To obtain the appropriate potential, the parameters V_0 and r_0 were varied accordingly so that the corresponding 1D BPM cross sections agree with those obtained using the AW potential parameters at higher energies [19]. The modified potential used for the CC calculations, and the corresponding uncoupled-barrier parameters are given in Table I. Using the modified potential parameters, the 1D BPM

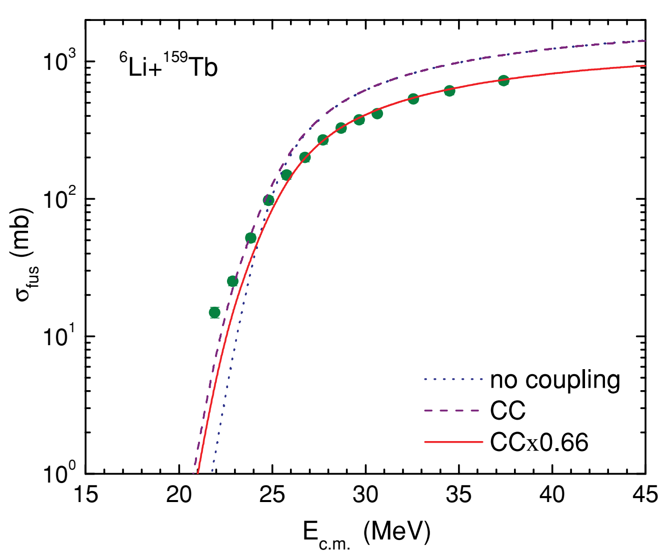

FIG. 3. (Color online) Complete fusion cross sections as a function of the center-of-mass energy for the reaction ^{6}Li + ^{159}Tb. The error bars indicate the total errors. The dotted and dashed lines show the uncoupled- and coupled-channel calculations, respectively, performed with the code CCFULL. The solid line is the coupled-channel calculation multiplied by a factor of 0.66.

TABLE I. The parameters for AW and modified CC potentials, along with the corresponding derived uncoupled-barrier parameters V_b, R_b, and $\hbar\omega$.

System	Potential	V_0 (MeV)	r_0 (fm)	a (fm)	V_b (MeV)	R_b (fm)	$\hbar\omega$ (MeV)
^{6}Li + ^{159}Tb	AW	46.40	1.18	0.62	24.89	10.60	4.85
	CC	128.0	0.98	0.85	24.48	10.53	4.15
^{7}Li + ^{159}Tb	AW	46.43	1.18	0.62	24.70	10.69	4.48
^{10}B + ^{159}Tb	AW	54.54	1.18	0.64	40.71	10.79	4.68
^{11}B + ^{159}Tb	AW	54.54	1.18	0.64	40.34	10.89	4.42

calculations were carried out using the code CCFULL, in the no-coupling limit, and the results are shown as the dotted line in Fig. 3. The CF cross sections at below-barrier energies are seen to be enhanced and the cross sections at above-barrier energies are found to be reduced compared to the 1D BPM calculations. The enhancement at below-barrier energies may be because of the fact that the target ^{159}Tb is a well-deformed nucleus.

The effect of target deformation on the fusion cross sections was calculated by including coupling to the ground-state rotational band of the target nucleus. As described in Ref. [19], for the odd-A nucleus ^{159}Tb, the excitation energies and deformation parameters were taken to be the averages of those of the neighboring even-even nuclei ^{158}Gd and ^{160}Dy. The energy states, in the ground-state rotational band of the corresponding average spectrum ($\beta_2 = 0.344$ [40] and $\beta_4 = +0.062$ [41]), up to 12^+ were included in the calculations. Projectile excitation was not included in the calculations. It needs to be mentioned here that ^{6}Li has a ground state with nonzero spin (1^+), a spectroscopic quadrupole moment of -0.082 fm^2, and an unbound first excited state (3^+) at 2.186 MeV. But coupling to the unbound first excited state of ^{6}Li with such ground-state properties, along with the rotational coupling to the target excited states, could not be included in the CCFULL calculations.

The dashed line in Fig. 3 shows the CC calculations that include rotational coupling to the inelastic states of the target. The calculations, though they reproduce the low-energy part of the data reasonably well, overestimate the high-energy part of the data. The small differences that can be seen at the lowest energy could be due to the projectile effect, which could not be considered in the calculations, as mentioned. At above-barrier energies, where coupling is not expected to play any significant role, the CF cross sections are found to be suppressed compared to the CC calculations.

As the CC model cannot yet separate CF and ICF, the measured CF cross sections can only be compared with the calculated total fusion cross sections. So in order to have an estimate of the extent of CF suppression compared to the total fusion cross sections, the CC calculations for ^{6}Li + ^{159}Tb were scaled so as to reproduce the high-energy part of the measured CF excitation function. Agreement could be achieved only if the calculated fusion cross sections are scaled by a factor of 0.66, and the resulting scaled calculations are shown in Fig. 3 as the solid line. The CF suppression factor (F_{CF}) for the system is thus 0.66 ± 0.05, where the uncertainty of $\pm 5\%$ has been estimated as resulting from the overall errors in the measured fusion cross sections. The CF suppression of $34\% \pm 5\%$ thereby obtained at above-barrier energies for ^{6}Li + ^{159}Tb agrees with the value reported for the heavier systems ^{6}Li + ^{209}Bi [14] and ^{6}Li + ^{208}Pb [16] and is also in close agreement with the suppression of $32\% \pm 5\%$ reported for ^{6}Li + ^{144}Sm [22].

V. COMPARISON OF SUPPRESSION WITH OTHER SYSTEMS

The F_{CF} for ^{6}Li-induced reactions on different targets are compared in Fig. 4(a), using the present data and those reported in the literature [14,16,22]. The dotted line has been drawn in the figure only to guide the eye. It appears that the F_{CF} for ^{6}Li-induced reactions are almost independent of the atomic number (Z_T) of the target nucleus, in the heavy-mass region. However, more values of F_{CF} for ^{6}Li-induced reactions, especially with targets of lower Z_T, are required before drawing any definite conclusion. Figure 4(b) compares the F_{CF} for the reactions ^{6}Li + ^{159}Tb, ^{7}Li + ^{159}Tb [19], and ^{10}B + ^{159}Tb [19] as a function of the α separation energies (SE$_\alpha$) of the projectiles. Like ^{6}Li + ^{159}Tb, a $\pm 5\%$ uncertainty has also been estimated for the F_{CF} of the ^{7}Li + ^{159}Tb and ^{10}B + ^{159}Tb reactions. The plot shows that there is a correlation between F_{CF} and SE$_\alpha$. But more such measurements, including reactions with unstable projectiles, are needed to understand the nature of the correlation.

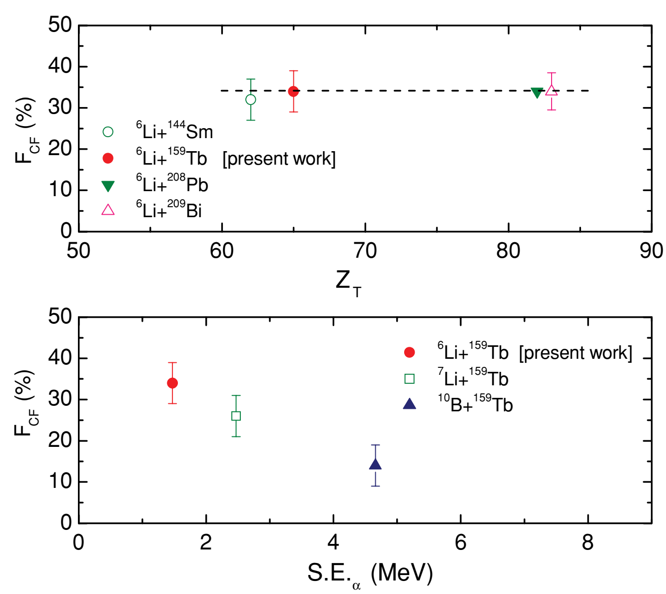

FIG. 4. (Color online) (a) CF suppression (%) as a function of the atomic number Z_T of the target for the ^{6}Li-induced reactions involving different targets. The reactions considered are ^{6}Li incident on ^{144}Sm [22], ^{159}Tb (present work), ^{208}Pb [16], and ^{209}Bi [14]. The dotted line is drawn to guide the eye. (b) CF suppression (%) as a function of the α separation energies (SE$_\alpha$) of the projectiles in reactions with the target ^{159}Tb. The reactions considered are ^{10}B + ^{159}Tb [19], ^{7}Li + ^{159}Tb [19], and ^{6}Li + ^{159}Tb (present work).

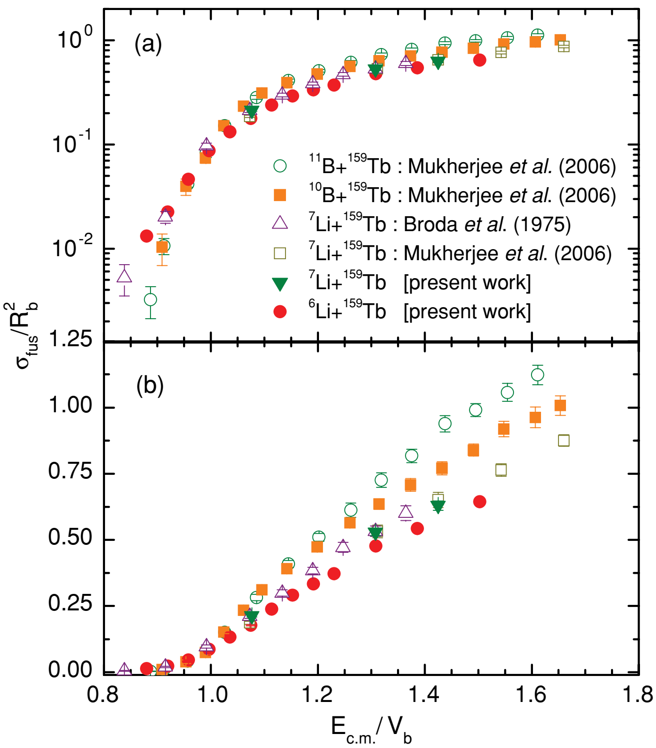

FIG. 5. (Color online) A comparison of the reduced complete fusion excitation functions for the systems ^{10,11}B + ^{159}Tb [19] and ^{7}Li + ^{159}Tb [19,36] with those of the present measurements for ^{6,7}Li + ^{159}Tb. The errors are statistical only.

Figure 5 compares the reduced fusion cross sections $\sigma_{\mathrm{fus}}/R_b^2$ as a function of $E_{\mathrm{c.m.}}/V_b$ for different projectiles with a logarithmic scale (a) and a linear scale (b). The parameters V_b and R_b used for the reduction are those deduced from the AW potentials, and are listed in Table I. The CF cross sections for ^{11,10}B + ^{159}Tb and ^{7}Li + ^{159}Tb were obtained from Refs. [19,36]. It can be seen from Fig. 5(a) that at the lowest energies the CF cross sections of ^{6,7}Li + ^{159}Tb are enhanced compared to those of the ^{10,11}B + ^{159}Tb reactions. This enhancement, which could be due to the effect of the projectiles ^{6,7}Li, was also observed while comparing the measurements with CCFULL calculations (Fig. 3 and Ref. [19]). For the reaction ^{6}Li + ^{159}Tb, this has already been discussed in Sec. IV. For the reaction ^{7}Li + ^{159}Tb, the deformation of ^{7}Li needs to be considered in the calculations [19], but both projectile and target deformations cannot be included simultaneously in the CCFULL calculations.

Figure 5(b) shows that as one moves from the projectile ^{11}B to ^{6}Li, i.e., as the projectile α breakup threshold decreases, the CF cross sections are observed to be more and more suppressed. A comparison with the CCFULL calculations has shown that the measured CF cross sections for ^{10}B + ^{159}Tb, ^{7}Li + ^{159}Tb [19], and ^{6}Li + ^{159}Tb are suppressed by ∼14%, ∼26%, and ∼34%, respectively. This certainly shows that the CF suppression is correlated with the α breakup threshold of the projectile. The lower the α breakup threshold, the larger the CF suppression. Thus CF suppression can be attributed to the loss of flux from the fusion channel due to the breakup of the loosely bound projectiles, and hence at least a major part of this suppression should be due to the ICF cross sections of the reactions. Also, if one looks carefully at Fig. 5(b), it appears that the higher the α breakup threshold of the projectile, the higher the energy where CF suppression starts. However, more such systematic measurements, especially with unstable beams, are required to confirm this observation.

VI. INCOMPLETE FUSION

In order to have a complete picture of the fusion process in the reaction ^{6}Li + ^{159}Tb, besides CF cross sections, it is also important to measure the ICF cross sections. As discussed in the previous section, a major part of the observed reduction in CF is expected to be due to the ICF process.

In the γ-ray spectra, besides the γ-ray lines of the Er nuclei resulting from CF, the γ-ray lines corresponding to Dy and Ho isotopes produced via the ICF processes were also observed. In the reaction ^{6}Li + ^{159}Tb, the Dy nuclei are produced by the capture of the lighter projectile fragment d following ^{6}Li breakup, by the target ^{159}Tb, and subsequent emission of neutrons. Similarly, the Ho nuclei are formed by the capture of the heavier projectile fragment α by ^{159}Tb, followed by neutron emission. The ICF cross sections are shown in Fig. 6. The cross sections of the ICF products were determined in a similar way as that for the CF residues. The αn, $\alpha 2n$, and $\alpha 3n$ channels, following the capture of d by ^{159}Tb, are seen to be the dominant ICF channels. On the other hand, only γ lines corresponding to a ^{161}Ho nucleus resulting from the α + ^{159}Tb ICF process, followed by $2n$ emission, could be identified in the spectra. However, the ICF contribution of ^{161}Ho, plotted in the figure, partly includes the contribution of ^{161}Ho produced via the EC decay of the ^{161}Er CF residue. Nevertheless, it is clear that the contribution of ^{161}Ho formed in the ICF process

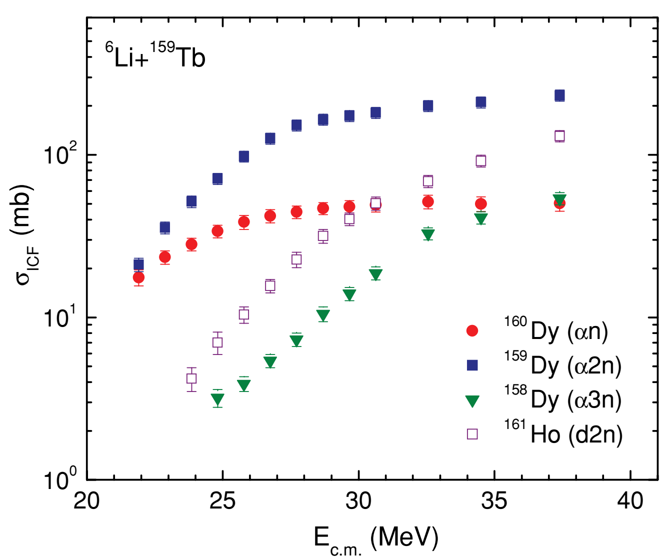

FIG. 6. (Color online) The ICF and/or transfer cross sections measured for the reaction ^{6}Li + ^{159}Tb. The cross sections corresponding to the αn, $\alpha 2n$, and $\alpha 3n$ channels, following d capture by the target, and the cross sections corresponding to the $d2n$ channel, following α capture by the target, are shown.

is relatively much less compared to Dy isotopes. A possible explanation of this could be given on the basis of the Q values of the reactions. It is to be noted that the Q value for the reaction ^{159}Tb(^{6}Li,α)^{161}Dy is +10.2 MeV, while it is −2.2 MeV for the reaction ^{159}Tb(^{6}Li,d)^{163}Ho. This indicates that the former channel corresponding to the ICF process, where the α particle is emitted and d is captured by the target, is more favored compared to the latter. Our measurements on the systems ^{7}Li + ^{159}Tb and ^{10}B + ^{159}Tb reported earlier [19] also showed similar results.

It needs to be mentioned here that the ICF cross sections for Dy isotopes also include contributions from the transfer of d from the projectile ^{6}Li to the higher excited states of the target, since in the present γ-ray measurement it was not possible to distinguish between the two events. Also, the single-proton stripping reaction ^{159}Tb(^{6}Li,^{5}He)^{160}Dy, with Q value +2.836 MeV, if it occurs, will lead to the same ^{160}Dy nucleus. Hence the contribution from ^{160}Dy nuclei via p transfer, if any, is also included in the αn channel cross section.

A careful study of Fig. 6 shows appreciable cross sections for Dy nuclei, even at energies below the barrier where CF shows no suppression (Fig. 3). This is perhaps because of the fact that at below-barrier energies, it is essentially the transfer of d to the unbound states of ^{159}Tb (a one-step process), followed by the emission of neutrons, that produces the Dy isotopes. In a simplistic picture, this can be understood by considering the optimum Q value (Q_{opt}) associated with a transfer reaction. The ground-state Q value (Q_{gg}) for the d-transfer reaction ^{159}Tb(^{6}Li,α)^{161}Dy is +10.2 MeV, and Q_{opt} for the transfer process, say at $E_{\mathrm{c.m.}} = 22$ and 25 MeV, are calculated [42] to be −7.1 MeV and −8.1 MeV, respectively. The excitation energy (ϵ^*) of ^{161}Dy to which the d transfer is energetically favored is given by $Q_{gg} - Q_{\mathrm{opt}}$. Thus at $E_{\mathrm{c.m.}} =$ 22 and 25 MeV, $\epsilon^* = 17.3$ and 18.3 MeV, respectively, thereby showing that the d transfer to ^{159}Tb will energetically favor the production of ^{161}Dy nuclei in the unbound states. Unlike transfers at below-barrier energies, the breakup fragments may not have sufficient energy to overcome the Coulomb barrier and to become captured by the target (a two-step process). In contrast, at above-barrier energies the breakup fragments will have sufficient energy to undergo further fusion with the target and hence at such energies the ICF (breakup-fusion) process, along with d transfer, leads to the production of Dy nuclei. It is mainly the ICF (breakup-fusion) yield (which could not be separated from the transfer yield in the present measurement) that contributes to the reduction of CF at above-barrier energies. A similar argument also holds true for the Ho nuclei. Unfortunately, only one Ho isotope, namely, ^{161}Ho, could be identified in the present work and that too had an admixture due to the contribution from ^{161}Ho nuclei resulting from the EC decay of the ^{161}Er residue. So nothing conclusive could be said about Ho nuclei. Detailed exclusive measurements aimed at disentangling ICF and transfer yields, though difficult, are indeed necessary to see how much of the reduction in CF is accounted for by the ICF process.

VII. SUMMARY

The CF cross sections for the reaction ^{6}Li + ^{159}Tb have been measured at energies around the Coulomb barrier, using the γ-ray method. CC calculations using the code CCFULL were carried out to calculate the total fusion cross sections. The calculated fusion cross sections had to be scaled by a factor of 0.66 ± 0.05 to reproduce the measured CF cross sections at above-barrier energies. The above-barrier CF suppression has been attributed to the breakup of the loosely bound ^{6}Li nucleus. The CF suppression of ∼34% for ^{6}Li + ^{159}Tb when compared to the values of ∼26% and ∼14% for ^{7}Li + ^{159}Tb and ^{10}B + ^{159}Tb [19], respectively, convincingly shows that CF suppression is correlated with the α separation energy of the projectile. The lower the α breakup threshold of the projectile, the larger the CF suppression. At energies below the barrier, the enhancement of CF cross sections could be reasonably well reproduced by considering the deformation of the target.

The nuclei produced via the ICF process in the reaction ^{6}Li + ^{159}Tb were also identified and their cross sections have been determined. Similar to ^{10}B + ^{159}Tb and ^{7}Li + ^{159}Tb [19], the present measurement also shows that the α-emitting channel is the favored ICF process in reactions of projectiles, having low α breakup thresholds, with a ^{159}Tb target.

At below-barrier energies, the Dy isotopes are primarily produced by the d transfer to the unbound states of ^{159}Tb, while at above-barrier energies both transfer and ICF processes contribute to their production.

Further investigation of the light particles emitted in reactions involving loosely bound projectiles, in conjunction with the results presented here, may lead to a better understanding of the mechanisms involved in such reactions.

ACKNOWLEDGMENTS

We are grateful to Professor B. K. Dasmahapatra for valuable discussions and advice at various stages of the work. We thank P. K. Das for his earnest technical help during the experiment. We would also like to thank the accelerator staff at the BARC-TIFR Pelletron Facility, Mumbai, for their untiring efforts in delivering the beams.

[1] M. Beckerman, Phys. Rep. **129**, 145 (1985); Rep. Prog. Phys. **51**, 1047 (1988).
[2] M. Dasgupta, D. J. Hinde, N. Rowley, and A. M. Stefanini, Ann. Rev. Nucl. Part. Sci. **48**, 401 (1998), and references therein.
[3] V. Fekou-Youmbi *et al.*, Nucl. Phys. A **583**, 811c (1995).
[4] Yu. E. Penionzhkevich, Nucl. Phys. A **588**, 259c (1995).
[5] A. S. Fomichev, I. David, Z. Dlouhy, S. M. Lukyanov, Yu. Ts. Oganessian, Yu. E. Penionzhkevich, V. P. Perelygin, N. K. Skobelev, O. B. Tarasov, and R. Wolski, Z. Phys. A **351**, 129 (1995).
[6] A. Yoshida *et al.*, Phys. Lett. B **389**, 457 (1996).
[7] K. E. Rehm *et al.*, Phys. Rev. Lett. **81**, 3341 (1998).
[8] J. J. Kolata *et al.*, Phys. Rev. Lett. **81**, 4580 (1998).

[9] M. Trotta *et al.*, Phys. Rev. Lett. **84**, 2342 (2000).
[10] C. Signorini *et al.*, Nucl. Phys. A **735**, 329 (2004).
[11] C. Signorini *et al.*, Eur. Phys. J. A **5**, 7 (1999).
[12] C. Signorini *et al.*, Eur. Phys. J. A **2**, 227 (1998).
[13] M. Dasgupta *et al.*, Phys. Rev. Lett. **82**, 1395 (1999).
[14] M. Dasgupta *et al.*, Phys. Rev. C **66**, 041602(R) (2002).
[15] V. Tripathi, A. Navin, K. Mahata, K. Ramachandran, A. Chatterjee, and S. Kailas, Phys. Rev. Lett. **88**, 172701 (2002).
[16] Y. W. Wu, Z. H. Liu, C. J. Lin, H. Q. Zhang, M. Ruan, F. Yang, Z. C. Li, M. Trotta, and K. Hagino, Phys. Rev. C **68**, 044605 (2003).
[17] M. Dasgupta *et al.*, Phys. Rev. C **70**, 024606 (2004).
[18] V. Tripathi, A. Navin, V. Nanal, R. G. Pillay, K. Mahata, K. Ramachandran, A. Shrivastava, A. Chatterjee, and S. Kailas, Phys. Rev. C **72**, 017601 (2005).
[19] A. Mukherjee *et al.*, Phys. Lett. B **636**, 91 (2006).
[20] P. R. S. Gomes *et al.*, Phys. Lett. B **634**, 356 (2006).
[21] P. R. S. Gomes *et al.*, Phys. Rev. C **73**, 064606 (2006).
[22] P. K. Rath *et al.*, Phys. Rev. C **79**, 051601 (2009).
[23] S. B. Moraes, P. R. S. Gomes, J. Lubian, J. J. S. Alves, R. M. Anjos, M. M. SantAnna, I. Padron, C. Muri, R. Ligouri Neto, and N. Added, Phys. Rev. C **61**, 064608 (2000).
[24] P. R. S. Gomes *et al.*, Phys. Lett. B **601**, 20 (2004).
[25] C. Beck *et al.*, Phys. Rev. C **67**, 054602 (2003).
[26] A. Mukherjee, U. D. Pramanik, M. S. Sarkar, A. Goswami, P. Basu, S. Bhattacharya, S. Sen, M. L. Chatterjee, and B. Dasmahapatra, Nucl. Phys. A **596**, 299 (1996).
[27] A. Mukherjee, U. D. Pramanik, S. Chattopadhyay, M. S. Sarkar, A. Goswami, P. Basu, S. Bhattacharya, M. L. Chatterjee, and B. Dasmahapatra, Nucl. Phys. A **635**, 305 (1998).
[28] A. Mukherjee, U. D. Pramanik, S. Chattopadhyay, M. S. Sarkar, A. Goswami, P. Basu, S. Bhattacharya, M. L. Chatterjee, and B. Dasmahapatra, Nucl. Phys. A **645**, 13 (1999).
[29] A. Mukherjee and B. Dasmahapatra, Phys. Rev. C **63**, 017604 (2000).
[30] A. Mukherjee, M. Dasgupta, D. J. Hinde, H. Timmers, R. D. Butt, and P. R. S. Gomes, Phys. Lett. B **526**, 295 (2002).
[31] M. Ray, A. Mukherjee, M. K. Pradhan, R. Kshetri, M. S. Sarkar, R. Palit, I. Majumdar, P. K. Joshi, H. C. Jain, and B. Dasmahapatra, Phys. Rev. C **78**, 064617 (2008).
[32] A. Mukherjee and M. K. Pradhan, Pramana **75**, 99 (2010).
[33] Computer code LAMPS (Linux Advanced Multiparameter System), [http://www.tifr.res.in/~pell/lamps.html].
[34] A. Gavron, Phys. Rev. C **21**, 230 (1980).
[35] J. B. Marion and F. C. Young, *Nuclear Reaction Analysis: Graphs and Tables* (North-Holland, Amsterdam, 1968), p. 38
[36] R. Broda, M. Ishihara, B. Herskind, H. Oeshler, S. Ogaza, and H. Ryde, Nucl. Phys. A **248**, 356 (1975).
[37] K. Hagino, N. Rowley, and A. T. Kruppa, Comput. Phys. Commun. **123**, 143 (1999).
[38] R. A. Broglia and A. Winther, *Heavy Ion Reactions* (Benjamin/Cummings, Reading, MA, 1981), Vol. 1.
[39] J. O. Newton, R. D. Butt, M. Dasgupta, D. J. Hinde, I. I. Gontchar, C. R. Morton, and K. Hagino, Phys. Lett. B **586**, 219 (2004).
[40] S. Raman, C. H. Malarkey, W. T. Milner, C. W. Nestor Jr., and P. H. Stelson, At. Data Nucl. Data Tables **36**, 1 (1987).
[41] P. Möller, J. R. Nix, W. D. Myers, and W. J. Swiatecki, At. Data Nucl. Data Tables **59**, 185 (1995).
[42] H. Morgenstern, W. Bohne, W. Galster, and K. Grabisch, Z. Phys. A **324**, 443 (1986).